Acta Cryst. (1999). A**55**, 48–57

The periodic average structure of particular quasicrystals

Walter Steurer* and Torsten Haibach

Laboratory of Crystallography, Swiss Federal Institute of Technology, CH-8092 Zurich, Switzerland.
E-mail: steurer@kristall.erdw.ethz.ch

(*Received 16 September 1997; accepted 20 May 1998*)

Abstract

The non-crystallographic symmetry of *d*-dimensional (*d*D) quasiperiodic structures is incompatible with lattice periodicity in *d*D physical space. However, *d*D quasiperiodic structures can be described as irrational sections of *n*D ($n > d$) periodic hypercrystal structures. By appropriate oblique projection of particular hypercrystal structures onto physical space, discrete periodic average structures can be obtained. The boundaries of the projected atomic surfaces give the maximum distance of each atom in a quasiperiodic structure from the vertices of the reference lattice of its average structure. These maximum distances turn out to be smaller than even the shortest atomic bond lengths. The metrics of the average structure of a 3D Ammann tiling, for instance, with edge lengths of the unit tiles equal to the bond lengths in elemental aluminium, correspond almost exactly to the metrics of face-centred-cubic aluminium. This is remarkable since most stable quasicrystals contain aluminium as the main constitutent. The study of the average structure of quasicrystals can be a valuable aid to the elucidation of the geometry of quasicrystal-to-crystal transformations. It can also contribute to the derivation of the physically most relevant Brillouin (Jones) zone.

1. Introduction

The concept of average structure (AS) is essential for the analysis and description of all kinds of real crystal structures. When looked at in detail, because of the existence of defects and thermal vibrations of the atoms, structures of real crystals are never periodic. In addition, structural disorder and/or superordering phenomena may be present in a crystal (*cf*. Jagodzinski & Frey, 1993, and references therein). The time and space average over a real structure is called the average structure. It corresponds to the ideal structure convoluted with the probability density function (p.d.f.) of the atoms. The lattice of an AS is called the reference lattice. The AS is the only structural information that can be obtained from a diffraction-data-based structure analysis restricted to Bragg reflections. The mapping of a real structure onto its AS is unidirectional only.

In the case of an incommensurately modulated structure (IMS) and of a composite structure (CS), averaging can be performed on two levels. Statistical static and dynamic structural fluctuations can be averaged as described above. The result is an ideal aperiodic crystal structure convoluted with the p.d.f. of the atoms, *i.e.* an aperiodic AS. Furthermore, by convenient projection, a periodic AS can be obtained from the aperiodic AS. For an IMS, the projection has to occur along the modulation wave vectors and, for a CS, onto the sublattices. All atomic positions of an IMS with displacive modulation can be obtained by bounded shifts from the corresponding positions of its AS. A one-to-one mapping is possible. In the case of a superstructure or an IMS with density modulation, the AS does not exhibit fully occupied atomic sites. If the modulation function is a statistical distribution function (as in most cases), a one-to-one mapping between the atomic sites of such an IMS and the reference lattice nodes of its AS is no longer possible.

For a quasicrystal (QC) with noncrystallographic symmetry, it is commonly assumed that no 'discrete' periodic average structure could exist. Discrete average structure means that the projection of an infinite aperiodic structure into one unit cell of the AS does not fill it densely. In the 1D quasiperiodic case, the only possible point-symmetry groups, $\bar{1}$ or 1, are crystallographic ones. It is clear that a 1D QC can also be described as an IMS. Consequently, 1D quasicrystals exhibit periodic average structures. Whether they are discrete or not depends on the properties of the 'atomic surfaces' (for a definition see §2). In the case of 2D or 3D quasiperiodic structures with noncrystallographic point symmetry, however, the possibility of discrete periodic average structures is not so obvious.

The problem of periodic components in quasicrystals has been studied for many years. Wolny & Lebech (1986) and Spal (1986) described icosahedral quasicrystals as complex composite crystals consisting of ten different modulated sublattices. Wolny (1993, and references therein) also performed reciprocal-space analysis investigating periodic components in the diffraction patterns of quasicrystals. Duneau & Oguey (1990, 1991) and Duneau (1991) demonstrated that periodic reference lattices generally exist under certain

ISSN 0108-7673

conditions concerning size and shape of atomic surfaces in the nD description. They derived as sufficient condition that the atomic surface must be a unit cell for a lattice in perpendicular space (Duneau, 1991). Then, a bounded one-to-one mapping of the vertices of the quasiperiodic structure to the vertices of the reference lattice is possible (Duneau & Oguey, 1990, 1991). In the case of more complex atomic surfaces, a decomposition into parallelepipeds, being again unit cells in perpendicular space, is proposed. Each of the resulting sublattices would again display a reference lattice.

The motivation for the present work stems from the study of geometrical aspects of quasicrystal-to-crystal phase transformations (*cf.* Honal *et al.*, 1998). The existence of an AS of a quasicrystal may also be important for the derivation of a physically relevant Brillouin or Jones zone (*cf.* Poon, 1992; LÏck & Kek, 1993). Since real quasicrystal structures display very complex atomic surfaces, a simple method should be developed to derive AS in a similar way as in the case of a disordered structure or an IMS. Thus, not the special cases where one-to-one mapping is possible, but the more realistic ones where one-to-one mapping is unfortunately not possible should be studied on model structures. The lack of the one-to-one mapping property between a quasicrystal structure and its approximant may be the origin of the inherent disorder observed after quasicrystal-to-crystal transformations.

The 1D, 2D and 3D quasiperiodic structures analysed in the following are model structures for the experimentally observed classes of stable quasicrystals. The average structures and their properties are discussed in direct as well as in reciprocal space. Background information on the quasiperiodic prototype structures analysed in the present paper as well as on the nD embedding method can be obtained, for instance, from Steurer & Haibach (1998) and Yamamoto (1996).

2. The average structure of the Fibonacci sequence

2.1. *Definitions*

The Fibonacci sequence (FS) is the classical example of a 1D quasiperiodic structure (*cf.* Janssen, 1986; Steurer & Haibach, 1998, and references therein). Starting with S, it can be obtained by iteratively applying the substitution rule $S \rightarrow L$, $L \rightarrow LS$. If one assigns a short interval to S and a long one to L, with $L = \tau S$ and $\tau = 2\cos(\pi/5) = 1.618$, a quasiperiodic sequence of vertices (quasilattice) results. The frequency of L tiles is τ-times larger than that of S tiles. 'Decoration' of the vertices with atoms represents the best-known example of a 1D quasiperiodic structure.

The Fibonacci sequence can also be generated by an irrational cut of a 2D hypercrystal structure with the 1D physical space (Fig. 1*a*). The 2D embedding space $\mathbf{V} = \mathbf{V}^{\parallel} \oplus \mathbf{V}^{\perp}$, consists of two orthogonal 1D subspaces, $\mathbf{V}^{\parallel}$ (physical space) and $\mathbf{V}^{\perp}$ (perpendicular space). A hypercrystal structure is described by a hyperlattice decorated with hyperatoms. The perpendicular space components of the hyperatoms are called atomic surfaces. The physical space components of the hyperatoms correspond to the real 3D atoms. In all our examples, however, we use 1D point atoms for simplicity. The 2D lattice is spanned by the basis vectors

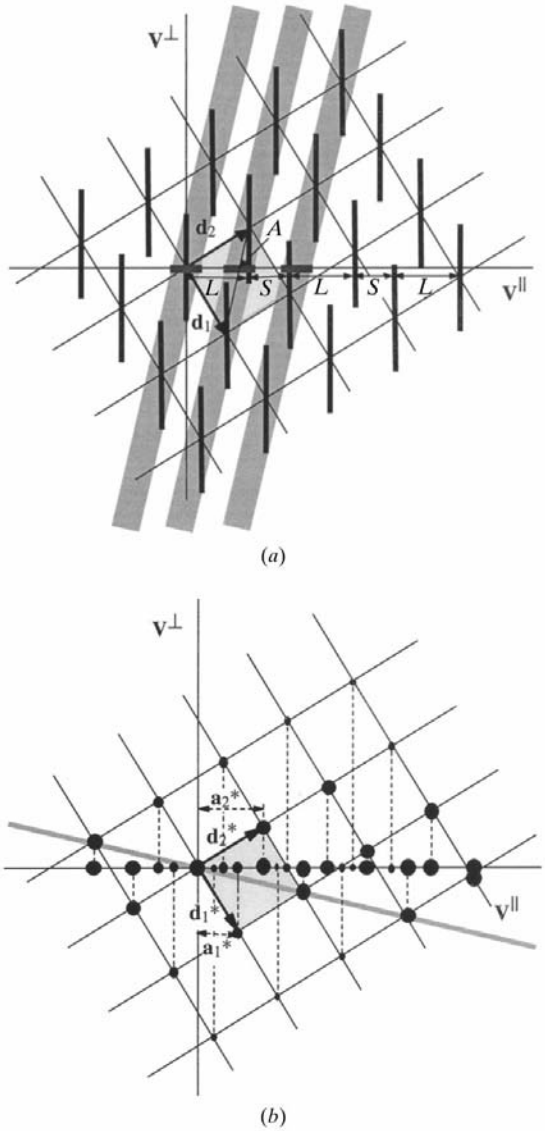

Fig. 1. (*a*) Direct- and (*b*) reciprocal-space representation of the 1D Fibonacci sequence in the 2D description. The grey bars indicate the projection direction of the atomic surfaces (thick line segements) in (*a*), and the reciprocal-lattice line containing the main reflections (full circles) in (*b*). The horizontal thick dark-grey bars in (*a*) represent the projected atomic surfaces. The unit-cell length of the average structure is marked by *A*.

$$\mathbf{d}_1 = \frac{1}{a^*(2+\tau)}\begin{pmatrix}1\\-\tau\end{pmatrix}_V, \qquad \mathbf{d}_2 = \frac{1}{a^*(2+\tau)}\begin{pmatrix}\tau\\1\end{pmatrix}_V \tag{1}$$

with a^* the length of the vector of the experimentally accessible reciprocal parallel space

$$a^* = |\mathbf{a}^*| = 1/[S(2+\tau)]. \tag{2}$$

Subscript V denotes vector components given on a Cartesian coordinate system in $\mathbf{V}$ space (V basis); subscript D will refer to the nD hypercrystal basis. The 2D square lattice is decorated by line segments (atomic surfaces). An atomic surface of such a canonical tiling results from the projection of one unit cell upon $\mathbf{V}^\perp$. The 2D hypercrystal structure is centrosymmetric. Shifting physical space along $\mathbf{V}^\perp$ leads to locally isomorphous homometric 1D quasiperiodic structures.

The point density $\rho_P^{\rm Fib}$ of the Fibonacci chain, *i.e.* the number of vertices per unit length, amounts to

$$\rho_P^{\rm Fib} = 1/a_{\rm av}^{\rm Fib} = a^*(2+\tau)/(3-\tau) = a^*\tau^2 \tag{3}$$

with the lattice parameter of the average structure

$$\begin{aligned} a_{\rm av}^{\rm Fib} &= \lim_{n\to\infty}[(mS+nL)/(m+n)] \\ &= \lim_{n\to\infty}[S(1+\tau n/m)/(1+n/m)] \\ &= S(1+\tau^2)/(1+\tau) = (3-\tau)S. \end{aligned} \tag{4}$$

In reciprocal space, the 1D diffraction pattern

$$M^* = \left\{\mathbf{H}^\parallel = \sum_{i=1}^{2} h_i\mathbf{a}_i^* | \mathbf{a}_1^* = \mathbf{a}^*, \mathbf{a}_2^* = \tau\mathbf{a}^*, h_i \in \mathbb{Z}\right\} \tag{5}$$

can be considered as projection of a 2D reciprocal lattice Σ^* onto physical space (Fig. 1*b*). The basis of Σ^* is given by

$$\mathbf{d}_1^* = a^*\begin{pmatrix}1\\-\tau\end{pmatrix}_V, \quad \mathbf{d}_2^* = a^*\begin{pmatrix}\tau\\1\end{pmatrix}_V. \tag{6}$$

2.2. *Average structure*

An appropriate AS of the Fibonacci sequence can be obtained by oblique projection of the atomic surfaces along $[\bar{1}\,1]_D$ onto physical space. The projection direction is equivalent to the wave vector of a saw-tooth modulation of an IMS. The projector applied on components can be written as

$$\begin{aligned} \pi^\parallel &= [\,1\;(3-2\tau)]_V \\ &= \{1/[a^*(2+\tau)]\}[(3-\tau)(3-\tau)]_D \end{aligned} \tag{7}$$

on V and D bases, respectively. The periodicity of the average structure $a_{\rm av}^{\rm Fib}$ becomes

$$a_{\rm av}^{\rm Fib} = \pi^\parallel\mathbf{d}_1 = (3-\tau)S. \tag{8}$$

Since the 2D hyperlattice of the FS is primitive and the atomic surface is a unit cell in $\mathbf{V}^\perp$, a bounded one-to-one mapping of the vertices of the FS onto the vertices of the reference lattice is possible (Duneau, 1991). Consequently, the period of the AS can also simply be derived from the condition that the densities of the quasiperiodic structure and its average structure have to be equal. Of course, there are an infinite number of different oblique projections leading to discrete average structures. The projection along $[\bar{1}\,1]_D$, however, is the only one yielding occupancy factors of the projected atomic surfaces equal to one. This is a necessary condition for a bounded one-to-one mapping of the quasiperiodic structure onto the periodic average structure. By the oblique projection, the atomic surfaces of length $(1+\tau)/[a^*(2+\tau)]$ are shrunk by a factor of $(2\tau-3)$. The packing density of the average structure, *i.e.* the ratio of the size of projected atomic surfaces to the AS lattice parameter, is $5^{-1/2} = 0.447$.

In 1D reciprocal space, the vector spanning the lattice of main reflections related to the average structure is given by $\mathbf{a}^{*\rm Fib}_{\rm av}\cdot\mathbf{a}^{\rm Fib}_{\rm av} = 1$. In 2D hyperspace, the reciprocal-lattice line containing the main reflections runs along $(1\,1)_D$ as given by the orthogonality relation

$$(-1\,1)_D\begin{pmatrix}h_1\\h_2\end{pmatrix}_D = 0 \rightarrow h_1 = h_2. \tag{9}$$

Thus, all reflections of type $(h\,h)$ are main reflections.

The weight of the average structure compared with the actual structure can be estimated by the ratio r_I of the sum of intensities of the main reflections to the sum of intensities of all reflections. For realistic conditions, r_I amounts to ~43.5% (X-ray diffraction, all vertices of the FS decorated with Al atoms, L = 4 Å, isotropic displacement parameter $B = 1$ Å^2, $0 \le \sin\theta/\lambda \le 1$ Å^{-1}, $-60 \le h_i \le 60$, $i = 1, 2$; 4385 reflections).

3. The average structure of the Penrose tiling

3.1. *Definitions*

A typical example of a 2D quasiperiodic structure with local fivefold symmetry is the Penrose tiling (PT) (*cf.* Penrose, 1974; Pavlovitch & Kleman, 1987; Steurer & Haibach, 1998, and references therein). It can be generated from two unit tiles: a skinny (acute angle $\alpha_s = \pi/5$) and a fat (acute angle $\alpha_f = 2\pi/5$) rhomb with equal edge lengths a_r and areas $A_s = a_r^2\sin(\pi/5)$, $A_f = a_r^2\sin(2\pi/5)$. The areas of these two unit tiles as well as their frequencies are both in the ratio 1 to τ.

In the nD approach, the Penrose tiling can be obtained as an irrational cut of a 4D hypercrystal structure with the 2D physical space (Fig. 2). The 4D embedding space $\mathbf{V} = \mathbf{V}^\parallel \oplus \mathbf{V}^\perp$ consists of the two

orthogonal 2D subspaces $\mathbf{V}^{\parallel}$ and $\mathbf{V}^{\perp}$. The 4D lattice is spanned by the basis vectors

$$\mathbf{d}_i = \frac{2}{5a^*} \begin{pmatrix} \cos(2\pi i/5) - 1 \\ \sin(2\pi i/5) \\ \cos(4\pi i/5) - 1 \\ \sin(4\pi i/5) \end{pmatrix}_V, \quad \text{with } i = 1, \ldots, 4. \quad (10)$$

a^* gives the length of the four reciprocal parallel space basis vectors which allow for indexing the diffraction pattern with integers. The 4D hyperrhombohedral lattice is decorated with four atomic surfaces of pentagonal shape. They occupy the special positions $p/5\,(1\,1\,1\,1)_D$, $p = 1, \ldots 4$, on the body diagonal. The pentagon radii are

$$\lambda_{1,4} = 2(2 - \tau)/5a^* \text{ and } \lambda_{2,3} = 2(\tau - 1)/5a^* \quad (11)$$

for the atomic surfaces with $p = 1, 4$ and $p = 2, 3$, respectively. Their orientations can be obtained from Fig. 2(*a*). The 4D structure is centrosymmetric.

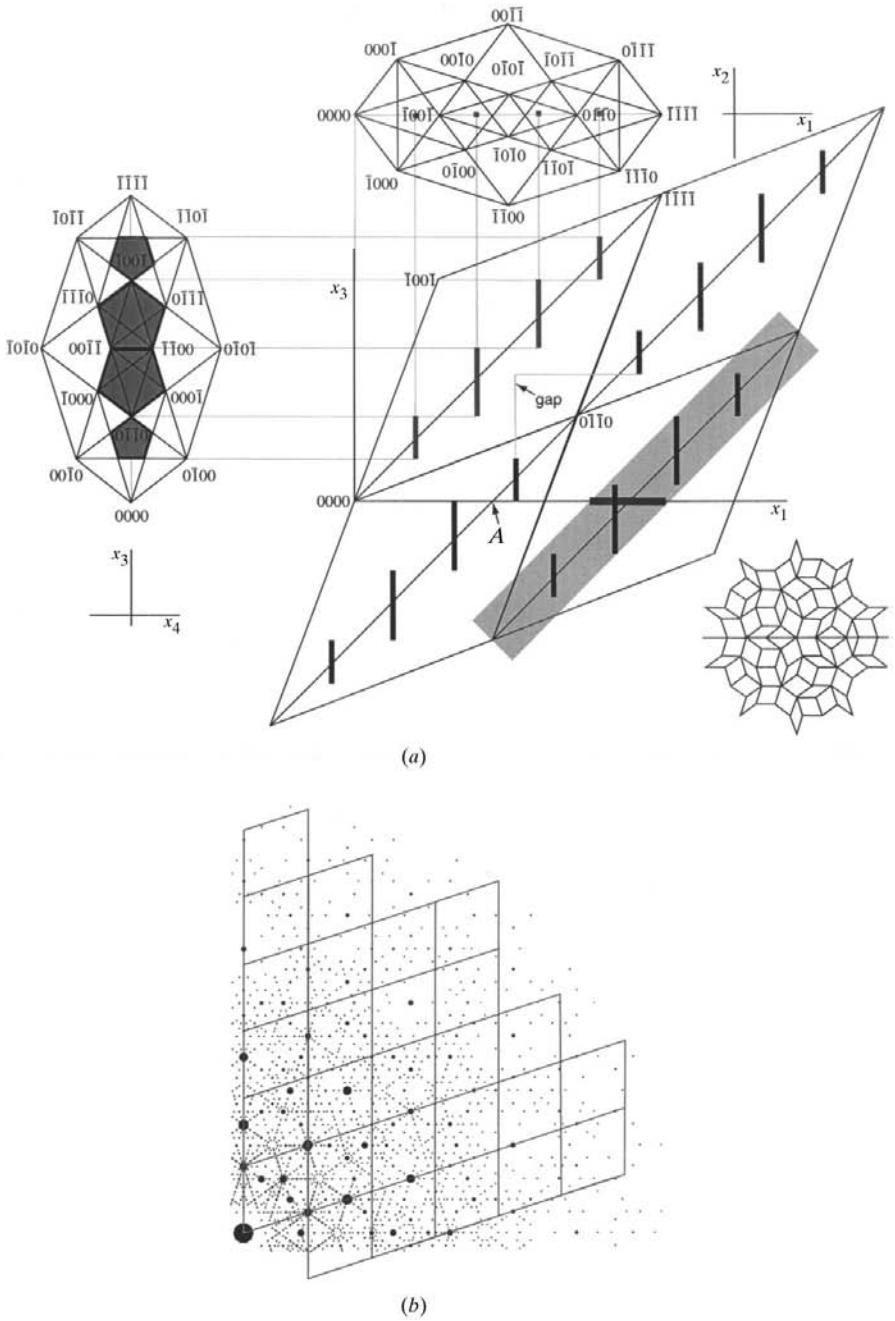

Fig. 2. (*a*) $(1\,0\,1\,0)_V$ section of the Penrose tiling in the 4D description. The projections of one 4D unit cell onto parallel space $(1\,1\,0\,0)_V$ and perpendicular space $(0\,0\,1\,1)_V$ are also shown. The atomic surfaces [line elements in the $(1\,0\,1\,0)_V$ section] projected upon $\mathbf{V}^{\perp}$ appear as regular pentagons. Upon $\mathbf{V}^{\parallel}$, they are projected to points. The direction of the oblique projection is marked by a grey strip. The image of the atomic surfaces projected within this strip is illustrated by a horizontal thick bar. The orientation of the $(1\,0\,1\,0)_V$ section with respect to the 2D Penrose tiling is indicated by a line in the lower right corner of the figure. The point marked *A* gives the dimension of the average unit cell along $(1\,0\,0\,0)_V$. Within the gap marked, no atomic surface on the particular diagonal is cut by physical space ($\mathbf{x}_1$). (*b*) Schematical diffraction pattern of the Penrose tiling (Al atoms, isotropic displacement parameter 1 Å^2, edge length of the Penrose unit rhombs, a_r = 4 Å). All reflections are shown within $10^{-4}\ |F(\mathbf{0})|^2 < |F(\mathbf{H})|^2 < |F(\mathbf{0})|^2$ and $0 \le |\mathbf{H}^{\parallel}| \le 2$ Å^{-1}. The main reflections corresponding to the average structure are located on the monoclinic lattice nodes. The size of the full circles is related to the respective reflection intensities.

The edge length a_r of a Penrose rhomb is related to the length a^* of the reciprocal-basis vectors by $a_r = 2\tau^2/5a^*$. The point density of a Penrose tiling can be derived from the ratio of the relative number of unit tiles in the tiling to their area

$$\begin{aligned}\rho_P^{\mathrm{PT}} &= (1+\tau)/\{a_r^2[\sin(\pi/5)+\tau\sin(2\pi/5)]\}\\ &= (5/2)(a^*)^2(2-\tau)^2\tan(2\pi/5).\end{aligned} \tag{12}$$

In reciprocal space, the 2D diffraction pattern

$$M^* = \left\{\mathbf{H}^{\parallel} = \sum_{i=1}^{4} h_i\mathbf{a}_i^* \middle| \mathbf{a}_i^* = a^*\begin{bmatrix}\cos(2\pi i/5)\\ \sin(2\pi i/5)\end{bmatrix}, h_i \in \mathbb{Z}\right\} \tag{13}$$

can be considered as a projection of a 4D reciprocal lattice Σ^* onto physical space (Fig. 2*b*). The basis of Σ^* is

$$\mathbf{d}_i^* = a^*\begin{bmatrix}\cos(2\pi i/5)\\ \sin(2\pi i/5)\\ \cos(4\pi i/5)\\ \sin(4\pi i/5)\end{bmatrix}_V, \quad \text{with } i = 1,\ldots,4. \tag{14}$$

3.2. *Average structure*

An appropriate average structure of the PT can be obtained by oblique projection of the atomic surfaces along $[1\,1\,1\,1]_D$ and $[4\,1\,1\,1]_D$ onto physical space (Fig. 2*a*). The projector

$$\begin{aligned}\pi^{\parallel} &= \begin{bmatrix}1 & 0 & \bar{1} & -\tau(3-\tau)^{1/2}\\ 0 & 1 & 0 & -\tau\end{bmatrix}_V\\ &= 2(5)^{1/2}/5a^*\begin{bmatrix}0 & (\tau-1)/2 & -(\tau+1)/2 & 1\\ 0 & \cos(\pi/10) & -\cos(\pi/10) & 0\end{bmatrix}_D\end{aligned} \tag{15}$$

maps the basis of the 4D lattice $\mathbf{d}_i$, $i = 1,\ldots,4$, onto a monoclinic reference lattice with basis

$$\begin{aligned}a_{1\,\mathrm{av}}^{\mathrm{PT}} &= \pi^{\parallel}(\mathbf{d}_2) = 2(5)^{1/2}/5a^*\begin{pmatrix}1\\0\end{pmatrix},\\ a_{2\,\mathrm{av}}^{\mathrm{PT}} &= \pi^{\parallel}(\mathbf{d}_4) = 2(5)^{1/2}/5a^*\begin{bmatrix}\sin(\pi/10)\\ \cos(\pi/10)\end{bmatrix},\\ \pi^{\parallel}(\mathbf{d}_1) &= \begin{pmatrix}0\\0\end{pmatrix}, \quad \pi^{\parallel}(\mathbf{d}_3) = -\pi^{\parallel}(\mathbf{d}_2) - \pi^{\parallel}(\mathbf{d}_4).\end{aligned} \tag{16}$$

The lattice parameters of the monoclinic average structure become

$$\begin{aligned}a_{1\,\mathrm{av}}^{\mathrm{PT}} &= a_{2\,\mathrm{av}}^{\mathrm{PT}} = |\pi^{\parallel}\mathbf{d}_2| = |\pi^{\parallel}\mathbf{d}_4| = (2/5a^*)(2\tau-1)\\ &= a_r(3-\tau)/\tau,\\ \alpha &= \measuredangle(\pi^{\parallel}\mathbf{d}_2, \pi^{\parallel}\mathbf{d}_4) = 2\pi/5.\end{aligned} \tag{17}$$

Since the symmetry of the average structure is not monoclinic but orthorhombic, a centred orthorhombic unit cell with lattice parameters

$$a_{1\,\mathrm{av}}^{\mathrm{PT}} = (3-\tau)a_r, \quad a_{2\,\mathrm{av}}^{\mathrm{PT}} = a_r(3-\tau)^{3/2}/\tau \tag{18}$$

can also be used.

The projector leaves all points of the physical space invariant (*i.e.* the vertices of the PT). Since each of those points results from a cut of the physical space with one particular atomic surface, it also fixes one point of this atomic surface. The centre of the atomic surface, which is always at a special position on a body diagonal $(1\,1\,1\,1)_D$, is projected upon a node of the monoclinic reference lattice. Consequently, the boundaries of the projected atomic surfaces give the limits for the maximum distance of a PT vertex from a reference lattice node. According to Fig. 3, this maximum distance is given by

$$\tau^2\lambda_2 = 2\tau^2(\tau-1)/5a^* = 2\tau/5a^* = a_r/\tau. \tag{19}$$

The oblique projection distorts the atomic surfaces elliptically (Fig. 3*a*), *i.e.* the circumcircles of the pentagonal atomic surfaces become ellipses. The long axis of each ellipse corresponds to an elongation of the circumcircle radius by a factor τ^2, the short axis to a contraction by $1/\tau$. The distances along the unit-cell edges remain unscaled. The packing density of the average structure, *i.e.* the ratio of the area of the projected atomic surfaces to the area of the monoclinic unit cell, is $2/(3\tau+1) = 0.342$.

A general 4D lattice node $(n_1\ n_2\ n_3\ n_4)_D$ is projected upon a node $(m_1\ m_2) = (-n_3+n_4\ n_2-n_3)_D$ of the monoclinic reference lattice. Consequently, all hyperatoms that differ only by vectors $(n_1\ n_2\ n_2\ n_2)$ are projected upon one another. This is shown schematically

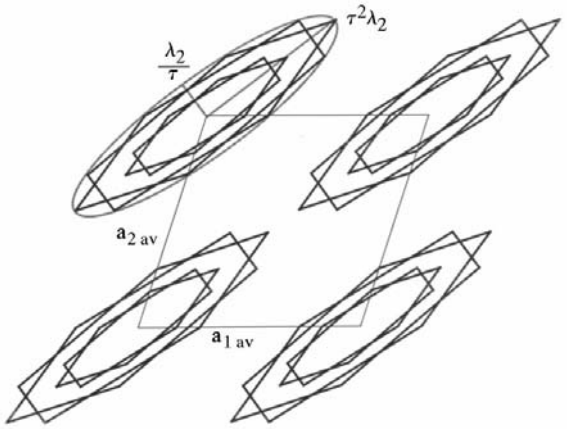

Fig. 3. One unit cell of the monoclinic average structure of the Penrose tiling decorated with the projected atomic surfaces. The half-axes of the ellipses that circumscribe the projected atomic surfaces are given. λ_2 denotes the radius of the large pentagonal atomic surface in the 4D description of the PT.

in Fig. 4(*a*). The occupancy factor of the averaged hyperatoms can be derived from the ratio of the total area of atomic surfaces in one unit cell spanned by the vectors $(1\,0\,0\,0)_D$ and $(1\,1\,1\,1)_D$ to the area of this unit cell (Fig. 4*a*). The occupancy factor is $(3-\tau)/\tau = 0.854$. It can also be calculated by considering the condition that the densities of the quasiperiodic structure and its average structure have to be equal.

There is, however, an overlap of one region D of each large pentagonal atomic surface and regions Q and K of the small ones (for a definition of D, Q and K see Jaric, 1986). This corresponds to the cases where the short diagonal of a skinny unit rhomb (connecting vertices of types D and K or D and Q) lies fully inside a projected hyperatom (Fig. 4*b*). The overlapping regions cover a fraction of $1/5\tau^2 = 0.076$ of the total area of the atomic surfaces. This corresponds to one fifth of the frequency of skinny rhombs in a Penrose tiling. Each doubly occupied averaged hyperatom is accompanied by two unoccupied ones. The frequency of singly occupied averaged hyperatoms is 0.7236, of doubly occupied ones 0.0652 and of unoccupied ones 0.2112. Each fat unit tile along all 'worms' (chains of fat and skinny PT unit rhombs with parallel edges) propagating perpendicular to the aforementioned short diagonals contains one empty averaged hyperatom. Thus, we have to sum up the frequencies of the vertices connected with such configurations (Henley, 1986):

$$\begin{aligned}&[(3-\tau)/5\tau](f_D + f_J + f_{S3} + 2f_K + 3f_{S4} + 5f_S + 5f_{S5})\\ &\quad = [(3-\tau)/5\tau](\tau^{-2} + \tau^{-3} + \tau^{-6} + 2\tau^{-5} + 3\tau^{-7}\\ &\qquad + 5^{1/2}\tau^{-5} + 5^{1/2}\tau^{-7})\\ &\quad = 0.2112 \end{aligned} \tag{20}$$

The worms propagating along the four other directions contain empty averaged hyperatoms only at the crossings with the first one.

The reciprocal-lattice plane containing the main reflections corresponding to the average structure is spanned by the reciprocal basis vectors

$$\begin{aligned}(\mathbf{a}_1^*)_{\rm av}^{\rm PT} &= a^*(3-\tau)^{1/2}\begin{bmatrix}\cos(\pi/10)\\ -\sin(\pi/10)\end{bmatrix}_V,\\ (\mathbf{a}_2^*)_{\rm av}^{\rm PT} &= a^*(3-\tau)^{1/2}\begin{pmatrix}0\\1\end{pmatrix}_V.\end{aligned} \tag{21}$$

All reflections of type $\mathbf{H} = (h_1\,h_2)_{\rm av} = [0\,h_2 - (h_1+h_2)\,h_1]_D$ are main reflections according to

$$\begin{pmatrix}0\\ h_2\\ -h_1-h_2\\ h_1\end{pmatrix}_D = \begin{pmatrix}0&0\\0&1\\-1&-1\\1&0\end{pmatrix}_{\rm av}\begin{pmatrix}h_1\\h_2\end{pmatrix}_{\rm av}. \tag{22}$$

The subscript av denotes components given on the basis defined by $\mathbf{a}_{i\rm av}^{\rm PT}$, $i = 1, 2$.

The weight of the average structure compared with that of the actual structure can be estimated by the ratio r_I of the sum of intensities of the main reflections to the sum of intensities of all reflections. For realistic conditions, r_I amounts to ~12.6% (X-ray diffraction, all vertices of the PT decorated with Al atoms, $a_r = 4$ Å, isotropic displacement parameter $B = 1$ Å^2, $0 \le \sin\theta/\lambda \le 1$ Å^{-1}, $-13 \le h_i \le 13$, $i = 0, \ldots, 4$ with $h_0 = -\sum_{i=1}^{4} h_i$; 182 972 reflections within 14 orders of magnitude). If the fact that at the same time this average structure is virtually present at five different orientations is taken into account, the weight increases to ~37.5% [for counting the (0 0 0 0) reflection only once].

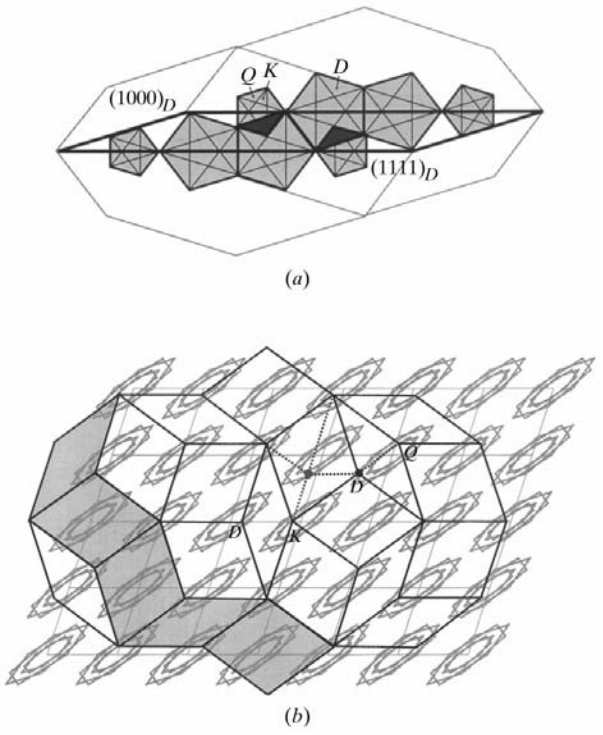

Fig. 4. (*a*) Two 4D unit cells of the PT related by the vector $(1\,0\,0\,0)_D$ projected upon the perpendicular space. The thick line marks one unit cell of the structure which is mapped into one averaged hyperatom by oblique projection. The overlapping regions of the atomic surfaces (of types D, K and Q) of the PT are shown in dark grey. (*b*) Monoclinic average structure superposed by a PT. Each vertex of the PT falls into one averaged hyperatom. The vertices marked D and Q share one averaged hyperatom. These vertices are generated from the regions shown in dark grey in (*a*). The vertex marked with the black full circle may jump to the vertex marked with the grey full circle to avoid doubly occupied averaged hyperatoms. Each fat unit tile along the grey-shaded worm contains one empty averaged hyperatom.

3.3. *The Penrose tiling and its fivefold twinned average structure*

Depending on the choice of the kernel for the oblique projection, one of five differently oriented symme-

trically equivalent monoclinic average structures results. We call the union of all five sets of monoclinic reference lattices a 5-lattice and of the average structures a 5-structure. In the 5-structure, each pair of vertices forming a short diagonal of a skinny rhomb falls inside one averaged hyperatom. No other vertex of the PT shares an averaged hyperatom with another one.

Each vertex $\boldsymbol{P}$ of the PT belongs to five intersecting averaged hyperatoms, which are assigned to five nodes $\boldsymbol{L}_i$, $i = 0, \ldots, 4$ of the 5-lattice (Fig. 5*a*), and it coincides

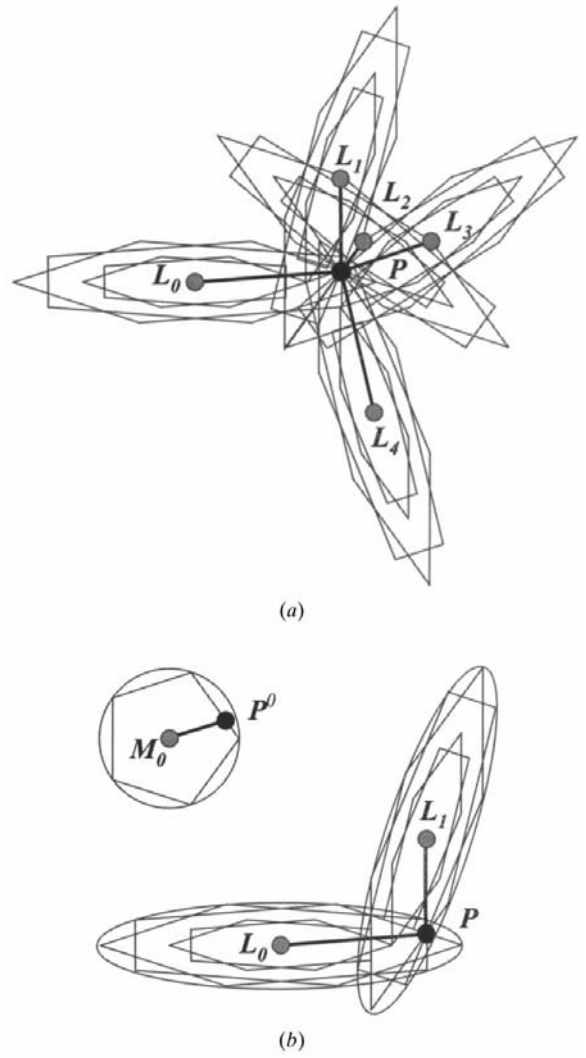

Fig. 5. (*a*) Set of five averaged hyperatoms resulting from five symmetrically equivalent oblique projections. The vertex $\boldsymbol{P}$ of the PT is the barycentre of the set $\boldsymbol{L}_i$, $i = 0, \ldots, 4$. The lattice nodes $\boldsymbol{L}_i$ belong to the five monoclinic reference lattices which are symmetrically equivalent under fivefold rotation. (*b*) The vertex $\boldsymbol{P}$ of the PT is generated by cutting the point $\boldsymbol{P}^0$ of a large pentagonal atomic surface with centre $\boldsymbol{M}_0$ by physical space. By oblique projection, the point $\boldsymbol{P}^0$ is mapped onto the point $\boldsymbol{P}$ and $\boldsymbol{M}_0$ onto $\boldsymbol{L}_0$. By changing the kernel of the projection matrix in an appropriate way, the resulting monoclinic average structure is rotated by $2\pi/5$.

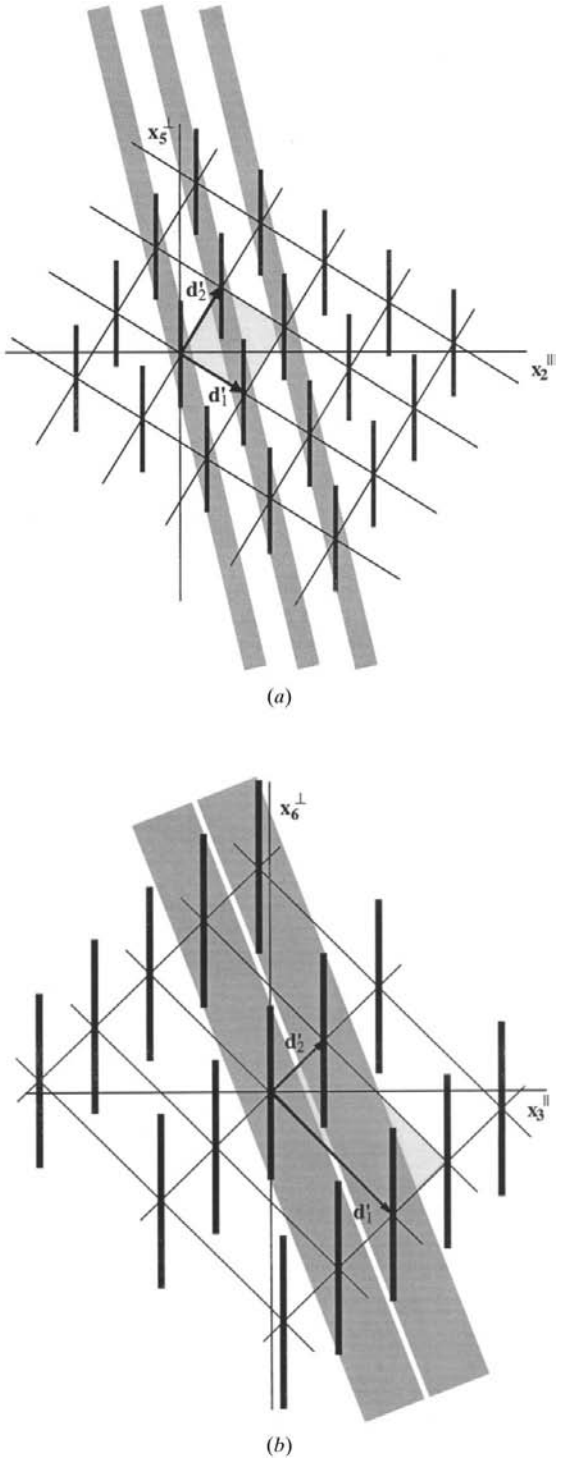

Fig. 6. Characteristic twofold (*a*) and fivefold (*b*) sections of the Ammann tiling in the 6D description. The vectors $\mathbf{d}'_1$ and $\mathbf{d}'_2$ correspond to the vectors $(000\,\bar{1}01)_D$ and $(01\bar{1}000)_D$ in (*a*), and to $(011111)_D$ and $(100000)_D$ in (*b*), respectively. The oblique projections in the respective sections are indicated by grey strips. In the case shown in (*a*), the projected atomic surfaces occupy much less space than in (*b*).

with the barycentre $\boldsymbol{B} = (1/5)\sum_{i=0}^{4} \boldsymbol{L}_i$. The vectors $\mathbf{s}_i = \boldsymbol{L}_i - \boldsymbol{B}$, $i = 0, \ldots, 4$, of a vertex $\boldsymbol{P}$ of the PT to the lattice nodes $\boldsymbol{L}_i$ are

$$\mathbf{s}_i = \begin{pmatrix} x_0 \\ y_0 \end{pmatrix} \begin{pmatrix} \cos(6\pi i/5) & -\sin(6\pi i/5) \\ \sin(6\pi i/5) & \cos(6\pi i/5) \end{pmatrix} \times \begin{pmatrix} \tau+1 & 0 \\ 0 & \tau-1 \end{pmatrix} \times \begin{pmatrix} \cos(2\pi i/5) & -\sin(2\pi i/5) \\ \sin(2\pi i/5) & \cos(2\pi i/5) \end{pmatrix}, \quad i = 0, \ldots, 4. \tag{23}$$

The vector $\boldsymbol{P}^0 = (x_0, y_0)$ points from the origin $\mathbf{M}_0$ of an atomic surface to that point on it that generates the vertex $\boldsymbol{P}$ of the PT (Fig. 5*b*).

The 5-lattice may be very helpful in the elucidation of the geometrical relationships between a quasicrystal structure and the domain structure formed during the transformation to the approximant. This has been demonstrated for the example of decagonal Al–Co–Ni (Honal *et al.*, 1998). In that case, the experimentally observed approximant of decagonal Al–Co–Ni is a superstructure of the average structure of decagonal Al–Co–Ni itself.

4. The average structure of the Ammann tiling

4.1. *Definitions*

The 3D analogue to the Penrose tiling is called Ammann tiling (AT) or 3D Penrose tiling (*cf.* Janssen, 1986; Levine & Steinhardt, 1986; Socolar & Steinhardt, 1986; Steurer & Haibach, 1998, and references therein). It can be constructed from two unit tiles: one prolate and one oblate rhombohedron with all edge lengths equal to a_r. Each face of such a rhombohedron is a rhomb with acute angles $\alpha_r = \arccos(5^{-1/2}) = 63.44°$. Their volumes are given by

$$V_p = (4/5)a_r^3 \sin(2\pi/5),\ V_o = (4/5)a_r^3 \sin(\pi/5) = V_p/\tau. \tag{24}$$

Their frequencies in the AT are in the ratio $\tau : 1$. The point density can be calculated by

$$\rho_p^{\mathrm{AT}} = (\tau+1)/(\tau V_p + V_o) = (\tau/a_r^3)\sin(2\pi/5). \tag{25}$$

The Ammann tiling can be obtained as an irrational cut of a 6D hypercubic crystal structure. The 6D embedding space $\mathbf{V} = \mathbf{V}^{\parallel} \oplus \mathbf{V}^{\perp}$ consists of two 3D orthogonal subspaces $\mathbf{V}^{\parallel}$ and $\mathbf{V}^{\perp}$. The 6D lattice is spanned by the basis vectors

$$\mathbf{d}_1 = \frac{1}{2a^*} \begin{pmatrix} 0 \\ 0 \\ 1 \\ 0 \\ 0 \\ 1 \end{pmatrix}_V, \qquad \mathbf{d}_i = \frac{1}{2a^*} \begin{pmatrix} \sin\theta\cos(2\pi i/5) \\ \sin\theta\sin(2\pi i/5) \\ \cos\theta \\ -\sin\theta\cos(4\pi i/5) \\ -\sin\theta\sin(4\pi i/5) \\ -\cos\theta \end{pmatrix}_V, \quad i = 2, \ldots 6;\ \theta = 63.44°. \tag{26}$$

The atomic surfaces of this canonical tiling result from the projection of the 6D unit cell upon the perpendicular space. They are of triacontahedral shape and occupy the hyperlattice nodes. The edge length of the rhombs covering such a triacontahedron is equivalent to $\pi^{\perp}(\mathbf{d}_i) = 1/2a^*$, the perpendicular-space component of the 6D basis vectors. The 6D structure is centrosymmetric.

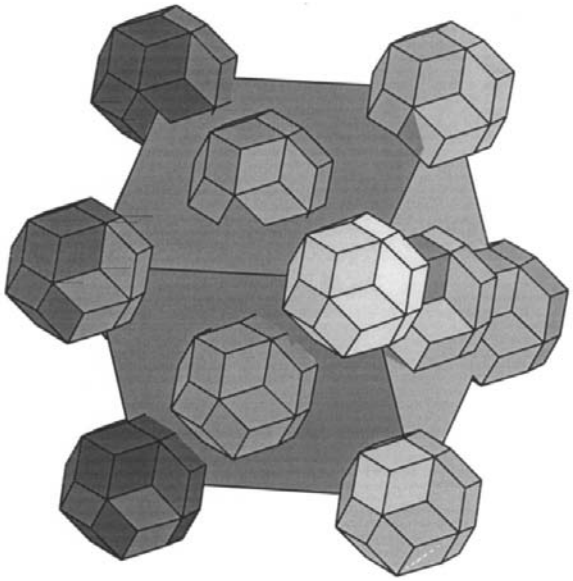

Fig. 7. Perspective view of one 3D unit cell of the average structure of the Ammann tiling. The face-centred unit cell is decorated by undistorted but shrunk triacontahedra resulting from the oblique projection.

4.2. *Average structure*

In Fig. 6*a*, the characteristic twofold section of the direct space of the Ammann tiling in the 6D representation is given. Twofold section means that a twofold axis of the 6D hyperlattice lies in this section. The grey bars indicate the oblique projection of the atomic surfaces along $(\bar{1}\,1\,1\,0\,1\,0)_D$, $(0\,1\,\bar{1}\,1\,0\,\bar{1})_D$ and $(\bar{1}\,0\,0\,1\,\bar{1}\,1)_D$ onto physical space by the projector

$$\pi^{\parallel} = \begin{pmatrix} 1 & 0 & 0 & 0 & 0 & -(2\tau-3) \\ 0 & 1 & 0 & 0 & 2\tau-3 & 0 \\ 0 & 0 & 1 & 2\tau-3 & 0 & 0 \end{pmatrix}_V$$
$$= \frac{1}{2a^*} \begin{pmatrix} -(2\tau-3) & -(\tau-1) & -(\tau-1) & 2-\tau & 1 & 2-\tau \\ 0 & \tan(\pi/5) & -\tan(\pi/5) & -\tan(\pi/5) & 0 & \tan(\pi/5) \\ 1 & 2-\tau & 2-\tau & \tau-1 & 2\tau-3 & \tau-1 \end{pmatrix}_D . \quad (27)$$

The lattice parameters of the resulting cubic average structure (Fig. 7) are

$$\boldsymbol{a}_{1\,\mathrm{av}}^{\mathrm{AT}} = \pi^{\parallel} \begin{pmatrix} 0 \\ \bar{1} \\ \bar{1} \\ 0 \\ 0 \\ 0 \end{pmatrix}_D = \frac{1}{a^*} \begin{pmatrix} \tau-1 \\ 0 \\ \tau-2 \end{pmatrix}_V ,$$
$$\boldsymbol{a}_{2\,\mathrm{av}}^{\mathrm{AT}} = \pi^{\parallel} \begin{pmatrix} 0 \\ 0 \\ 0 \\ \bar{1} \\ 0 \\ 1 \end{pmatrix}_D = \frac{1}{a^*} \begin{pmatrix} 0 \\ \tan(\pi/5) \\ 0 \end{pmatrix}_V , \quad (28)$$
$$\boldsymbol{a}_{3\,\mathrm{av}}^{\mathrm{AT}} = \pi^{\parallel} \begin{pmatrix} \bar{1} \\ 0 \\ 0 \\ 0 \\ \bar{1} \\ 0 \end{pmatrix}_D = \frac{1}{a^*} \begin{pmatrix} \tau-2 \\ 0 \\ 1-\tau \end{pmatrix}_V ,$$
$$a_{1\,\mathrm{av}}^{\mathrm{AT}} = a_{2\,\mathrm{av}}^{\mathrm{AT}} = a_{3\,\mathrm{av}}^{\mathrm{AT}} = [\tan(\pi/5)]/a^* = 2a_r \tan(\pi/5).$$

The projected basis vectors $\mathbf{d}_i$, $i = 1, \ldots, 6$, centre the faces of the cubic unit cell. Thus we obtain a face-centred-cubic average structure.

The projected atomic surfaces are of regular triacontahedral shape and by a factor $\cos\varphi = 0.230$, $\varphi = \arctan(\tau^3)$, smaller than the original ones. With the boundaries of the projected atomic surfaces also the limit for the maximum distance of an AT vertex from a reference lattice node is given by $\tau a_r \cos\varphi$. With the constraint of equal densities of the quasiperiodic structure and its average structure, an occupancy factor of $5/(2\tau+1) = 1.180$ results.

It follows from the projection of a general 6D lattice node

$$\pi^{\parallel}(n_1\,n_2\,n_3\,n_4\,n_5\,n_6)_D$$
$$= \frac{\tau-1}{2} \begin{pmatrix} (2-\tau)[(-n_2-n_3+n_4+2n_5+n_6)\tau \\ \quad -n_1-n_2-n_3+n_5] \\ (3-\tau)^{1/2}/\tau(n_2-n_3-n_4+n_6) \\ (2-\tau)[(2n_1+n_2+n_3+n_4+n_6)\tau \\ \quad +n_1+n_4+n_5+n_6] \end{pmatrix}_{\mathrm{av}} \quad (29)$$

that all 6D lattice nodes differing only in vectors $(n_1\,n_2\,n_3\,n_4\,n_5\,n_6)_D$ with $n_1+n_3+n_4 = 0, n_2-n_4-n_5 = 0$ and $n_1+n_2+n_6 = 0$ are projected onto the same averaged hyperatoms. Each triacontahedron overlaps with eight surrounding ones in volumes corresponding to one oblate rhombohedron in each case. For example, the cubic unit cell spanned by the vectors $(\bar{1}\,1\,1\,0\,1\,0)_D$, $(0\,1\,\bar{1}\,1\,0\,\bar{1})_D$ and $(\bar{1}\,0\,0\,1\,\bar{1}\,1)_D$ contains one triacontahedron at the eight corners and one in the body centre $(\bar{1}\,1\,0\,1\,0\,0)_D$. Since the cubic unit cell contains in total 20 prolate and 12 oblate rhombohedra, the eight overlapping oblate rhombohedra correspond to a fraction $2/(5\tau+3) = 0.180$. This means that 82% of all averaged atomic surfaces contain just one vertex of the Ammann tiling and 18% contain pairs of two vertices. These vertex pairs form the short diagonal of the oblate unit rhombohedra.

In a realistic quasicrystal structure model, the short diagonal of the oblate rhombohedra could only be alternately occupied if the edge length a_r of the unit tiles corresponds to the bond length. Thus, a realistic quasicrystal structure would not show the problem of an occupancy factor of the averaged hyperatoms larger than one. If the vertices of the AT are decorated with aluminium atoms, giving $a_r = 2.864$ Å (*i.e.* the bond length in elemental aluminium), the average structure would have lattice parameters $a_{i\,\mathrm{av}}^{\mathrm{AT}} = 2a_r \tan(\pi/5) = 4.161$ Å, compared with 4.045 Å for elemental aluminium. The maximum distance of a vertex of the AT from a lattice point of the average structure would be $\tau a_r \cos\varphi = 1.066$ Å.

The packing density of the average structure, *i.e.* the ratio of the volume of the projected atomic surfaces to the area of the cubic unit cell, is calculated as

$$4\tau \cos\varphi \sin(2\pi/5)/[\tan(\pi/5)]^3 = 0.195. \quad (30)$$

The characteristic fivefold section is given in Fig. 6(*b*). The oblique projection along the direction indicated by the grey bars and along two other symmetrically equivalent directions leads to a rhombohedral AS. Its packing density, however, is much higher than that of the face-centred-cubic AS.

The reciprocal lattice corresponding to the AS is spanned by the reciprocal basis vectors

$$
\begin{aligned}
(\boldsymbol{a}_1^*)_{\rm av}^{\rm AT} &= a^* \tan\frac{3\pi}{10}\begin{pmatrix}\cos(\theta/2)\\ 0\\ -\sin(\theta/2)\end{pmatrix}_V,\\
(\boldsymbol{a}_2^*)_{\rm av}^{\rm AT} &= a^* \tan\frac{3\pi}{10}\begin{pmatrix}0\\ 1\\ 0\end{pmatrix}_V,\\
(\boldsymbol{a}_3^*)_{\rm av}^{\rm AT} &= a^* \tan\frac{3\pi}{10}\begin{pmatrix}-\sin(\theta/2)\\ 0\\ -\cos(\theta/2)\end{pmatrix}_V.
\end{aligned}
\tag{31}
$$

They are by a factor τ^2 larger than the reciprocal basis vectors of the cubic setting which can be alternatively used for indexing the icosahedral phase (setting 2 of Steurer & Haibach, 1998). All reflections of type

$$
\begin{aligned}
\mathbf{H} &= (h_1\ h_2\ h_3)_{\rm av}\\
&= 1/2[(-h_1+h_3)(-h_1+h_2)(-h_1-h_2)(-h_2+h_3)\\
&\quad (h_1+h_3)(h_2+h_3)]_D
\end{aligned}
$$

are main reflections according to

$$
\frac{1}{2}\begin{pmatrix}-h_1+h_3\\ -h_1+h_2\\ -h_1-h_2\\ -h_2+h_3\\ h_1+h_3\\ h_2+h_3\end{pmatrix}_D = \frac{1}{2}\begin{pmatrix}-1 & 0 & 1\\ -1 & 1 & 0\\ -1 & -1 & 0\\ 0 & -1 & 1\\ 1 & 0 & 1\\ 0 & 1 & 1\end{pmatrix}_{\rm av}\begin{pmatrix}h_1\\ h_2\\ h_3\end{pmatrix}_{\rm av}. \tag{32}
$$

The subscript av denotes components given on the basis defined by $\boldsymbol{a}_{i\,\rm av}^{\rm AT}$, $i = 1, \ldots, 3$.

The weight of the average structure compared with the actual structure can be estimated by the ratio r_I of the sum of intensities of the main reflections to the sum of intensities of all reflections. For experimental conditions, r_I amounts to ~3.8% (X-ray diffraction, all vertices of the PT decorated with Al atoms, $a_r = 4$ Å, isotropic displacement parameter $B = 1$ Å^2, $0 \le \sin\theta/\lambda \le 1$ Å^{-1}, $|\mathbf{H}^{\perp}| \le 0.5$ Å^{-1}, $-6 \le h_i \le 6$, $i = 1, \ldots, 6$; 321 862 reflections). Taking into account that this average structure is virtually present at 20/8 different orientations at the same time, the weight increases to ~10.8% [for counting the 0 0 0 0 reflection only once].

5. Conclusions

It has been demonstrated that for the three prototypes of quasicrystal structures, the 1D Fibonacci sequence, the 2D Penrose tiling and the 3D Ammann tiling, discrete periodic average structures exist. The method proposed here for the derivation of AS by oblique projection is well suited for arbitrarily complex atomic surfaces and is easy to apply. A bi-unique mapping of the vertices of the quasiperiodic structure onto the averaged atomic surfaces of the AS has only be found in the case of the 1D FS. For 2D PT and 3D AT, only a unique mapping is possible. Thus, the 1D FS exhibits an AS in a similar way to a displacively modulated structure. 2D PT and 3D AT resemble modulated structures with both a density (*i.e.* ordering of vacancies and atoms) and a displacement modulation. The physical relevance of such an AS depends on size, occupancy factor and packing density of the projected atomic surfaces which give the limit for the distance of actual atoms from the nearest lattice point of the average structure.

We would like to acknowledge financial support by the Swiss National Science Foundation contracts 21-40249.94 and 20-46717.96.

References

Duneau, M. (1991). *Methods of Structural Analysis of Modulated Structures and Quasicrystals*, edited by J. M. PÅrez-Mato, F. J. ZÇ·iga & G. Madariaga, pp. 185–202. Singapore: World Scientific.

Duneau, M. & Oguey, C. (1990). *J. Phys. (France)*, **51**, 5–19.

Duneau, M. & Oguey, C. (1991). *J. Phys. A Math. Gen.* **24**, 461–475.

Henley, C. L. (1986). *Phys. Rev. B*, **34**, 797–816.

Honal, M., Haibach, T. & Steurer, W. (1998). *Acta Cryst.* A**54**, 374–387.

Jagodzinski, H. & Frey, F. (1993). *International Tables for Crystallography*, Vol. B, edited by U. Shmueli, Section 4.2. Dordrecht: Kluwer Academic Publishers.

Janssen, T. (1986). *Acta Cryst.* A**42**, 261–271.

Jaric, M. V. (1986). *Phys. Rev. B*, **34**, 4685–4698.

Levine, D. & Steinhardt, P. (1986). *Phys. Rev. B*, **34**, 596–616.

Lück, R. & Kek, S. (1993). *J. Non-Cryst. Solids*, **153&154**, 329–333.

Pavlovitch, A. & Kleman, M. (1987). *J. Phys. A Math. Gen.* **20**, 687–702.

Penrose, R. (1974). *Bull. Math. Appl.* **10**, 266–271.

Poon, S. J. (1992). *Adv Phys.* **41**, 303–363.

Socolar, J. E. S. & Steinhardt, P. (1986). *Phys. Rev. B*, **34**, 617–647.

Spal, R. D. (1986). *Phys. Rev. Lett.* **56**, 1823–1826.

Steurer, W. & Haibach, T. (1998). *International Tables for Crystallography*, Vol. B, 2nd ed., edited by U. Shmueli, Section 4.6. Dordrecht: Kluwer Academic Publishers. In the press.

Wolny, J. (1993). *J. Non-Cryst. Solids*, **153&154**, 293–297.

Wolny, J. & Lebech, B. (1986). *J. Phys. C Solid State Phys.* **19**, L161–L167.

Yamamoto, A. (1996). *Acta Cryst.* A**52**, 509–560.